



Contents lists available at SciVerse ScienceDirect

Science of the Total Environment

journal homepage: www.elsevier.com/locate/scitotenv

Mercury cycling in agricultural and managed wetlands of California, USA: Seasonal influences of vegetation on mercury methylation, storage, and transport

Lisamarie Windham-Myers^{a,*}, Mark Marvin-DiPasquale^a, Evangelos Kakouros^a, Jennifer L. Agee^a, Le H. Kieu^a, Craig A. Stricker^b, Jacob A. Fleck^c, Josh T. Ackerman^d

^a U.S. Geological Survey, Western Region Bureau of Regional Research, 345 Middlefield Road, MS 480, Menlo Park, CA, 94025, USA

^b U.S. Geological Survey, Fort Collins Science Center, Building 21, MS 963, Denver, CO, 80225, USA

^c U.S. Geological Survey, California Water Science Center, 6000J St, Placer Hall, Sacramento, CA, 95819, USA

^d U.S. Geological Survey, Western Ecological Research Center, Dixon Field Station, 800 Business Park Drive, Suite D, Dixon, CA, 95620, USA

HIGHLIGHTS

- Seasonal biomass and Hg, MeHg, C, and N composition were investigated for rice production.
- Seasonal biomass and Hg, C, and N composition influenced MeHg biogeochemical cycling.
- Decaying litter from rice residue also impacted pore-water acetate and MeHg production.
- Temporary storage of MeHg in plants and soils occurred in the summer due to low hydrologic export.
- MeHg accumulation in rice seeds may pose a risk to overwintering waterfowl in central CA.

ARTICLE INFO

Article history:

Received 29 July 2012

Received in revised form 6 May 2013

Accepted 12 May 2013

Available online xxx

Editor: Mae Sexauer Gustin

Keywords:

Methylmercury

Rice

Root

Biomass

Bioaccumulation

Litter

ABSTRACT

Plants are a dominant biologic and physical component of many wetland capable of influencing the internal pools and fluxes of methylmercury (MeHg). To investigate their role with respect to the latter, we examined the changing seasonal roles of vegetation biomass and Hg, C and N composition from May 2007–February 2008 in 3 types of agricultural wetlands (domesticated or white rice, wild rice, and fallow fields), and in adjacent managed natural wetlands dominated by cattail and bulrush (tule). We also determined the impact of vegetation on seasonal microbial Hg methylation rates, and Hg and MeHg export via seasonal storage in vegetation, and biotic consumption of rice seed. Despite a compressed growing season of ~3 months, annual net primary productivity (NPP) was greatest in white rice fields and carbon more labile (leaf median C:N ratio = 27). Decay of senescent litter (residue) was correlated with microbial MeHg production in winter among all wetlands. As agricultural biomass accumulated from July to August, THg concentrations declined in leaves but MeHg concentrations remained consistent, such that MeHg pools generally increased with growth. Vegetation provided a small, temporary, but significant storage term for MeHg in agricultural fields when compared with hydrologic export. White rice and wild rice seeds reached mean MeHg concentrations of 4.1 and 6.2 ng g_{dw}⁻¹, respectively. In white rice and wild rice fields, seed MeHg concentrations were correlated with root MeHg concentrations ($r = 0.90$, $p < 0.001$), suggesting transport of MeHg to seeds from belowground tissues. Given the proportionally elevated concentrations of MeHg in rice seeds, white and wild rice crops may act as a conduit of MeHg into biota, especially waterfowl which forage heavily on rice seeds within the Central Valley of California, USA. Thus, while plant tissues and rhizosphere soils provide temporary storage for MeHg during the growing season, export of MeHg is enhanced post-harvest through increased hydrologic and biotic export.

© 2013 Published by Elsevier B.V.

1. Introduction

Plant biomass can be an important factor in elemental cycling within wetland ecosystems (e.g. Brisson and Chazarenc, 2008). Biogeochemical feedbacks, direct or indirect, often involve microbial processes (e.g. Lamers et al., 2012), and may be immediate (e.g. through

* Corresponding author. Tel.: +1 650 329 4447; fax: +1 650 329 4463.

E-mail addresses: lwindham@usgs.gov (L. Windham-Myers), mmarvin@usgs.gov (M. Marvin-DiPasquale), kakouros@usgs.gov (E. Kakouros), jagee@usgs.gov (J.L. Agee), lkieu@usgs.gov (L.H. Kieu), cstricker@usgs.gov (C.A. Stricker), jafleck@usgs.gov (J.A. Fleck), jackerman@usgs.gov (J.T. Ackerman).

metabolic and hydraulic activity in the rhizosphere) or lagged (e.g. through litter accrual and decomposition; e.g. Hall et al., 2004; Rocha et al., 2008). Roots interact with microbial communities in rhizosphere soils within short time frames (seconds–days), typically by influencing the quality and supply of dissolved organic carbon (e.g. Hines et al., 1994; Cheng et al., 2003), the availability of electron acceptors (e.g. Lee et al., 1999), and/or nutrient or contaminant concentrations and speciation (e.g. Jacob and Otte, 2003).

Whereas metabolic processes (photosynthesis and respiration) influence microbial activity directly through carbon and oxygen dynamics (e.g. Ehrenfeld et al., 2005), plant biomass provides temporary storage of elements and also alters physical processes, such as water flow (e.g. Sereno and Stacey, 2002) and radiation exchange (e.g. Wollenberg and Peters, 2009). Mercury is taken up into (or onto) leaf tissue primarily through atmospheric exchange, depending on aquatic or atmospheric concentration gradients (e.g. Leonard et al., 1998; Erickson and Gustin, 2004; Fay and Gustin, 2007; Stamenkovic and Gustin, 2009). In contrast, methylmercury (MeHg) appears to be primarily taken up through roots (e.g. Schwesig and Krebs, 2003; Zhang et al., 2010). The distribution of MeHg within plants varies by species, tissue type, and physiological conditions (e.g. Patra and Sharma, 2000; Rothenberg et al., 2012), and this may have important ramifications on biotic Hg exposure. Movement into leaf tissues may provide a large seasonal storage term within wetlands, thus reducing aquatic concentrations and export of THg and MeHg to downstream environments (Marchand et al., 2010). The observed accumulation of MeHg transfer into seed tissues, of domesticated rice (*Oryza sativa*, hereafter referred to as white rice) (cf. Zhang et al., 2010), could enhance MeHg exposure to humans (Feng et al., 2008) or wildlife with seed-based diets, such as waterfowl who forage heavily on rice seeds during winter (Miller, 1987). Herein, we measured plant biomass, structure, and elemental (Hg, MeHg, C, and N) composition for dominant plant species growing in agricultural and naturally-vegetated wetlands, and assessed the extent to which vegetation may affect seasonal Hg dynamics of methylation, storage, and exposure to wildlife with seed-based diets.

Agricultural wetlands, such those cropped with white rice and wildrice (*Zizania palustris*), are a globally significant land use (Mitsch et al., 2010) with sediment conditions that are often amenable to methylation of mercury (Hg, Rothenberg and Feng, 2012; Marvin-DiPasquale et al., this issue). The fate of MeHg produced in agricultural wetland sediment may include fish and invertebrate uptake (Ackerman and Eagles-Smith, 2010; Ackerman et al., 2010), hydrologic export (Bachand et al., this issue-b), in situ photodemethylation (Fleck et al., in press), and in-field storage due to sediment and/or rhizosphere sequestration and tissue uptake. Physical retention in rhizosphere soils may limit export. Transpiration through white rice and wild rice leaf tissue at the height of the growing season can dominate water flux from agricultural systems (e.g. Brouder and Volenec, 2008; Bachand et al., this issue-a).

MeHg production was hypothesized to be high in agricultural wetlands of the Yolo Bypass, California, USA due to 1) elevated concentrations of legacy Hg (Springborn et al., 2011), 2) biannual flooding, and dessication associated with planting and harvesting cycles (Marvin-DiPasquale et al., this issue), and 3) significant availability of labile carbon from agricultural crops (Windham-Myers et al., 2009). While estimated rates of sediment MeHg production were generally high during summer ($5\text{--}89\text{ pg g}^{-1}\text{ d}^{-1}$, Marvin-DiPasquale et al., this issue), MeHg was not necessarily exported from all fields. As shown in Bachand et al. (this issue-b), MeHg load estimates were negative (import) to small (median = $2.8\text{ ng m}^{-2}\text{ d}^{-1}$) in the growing season compared to the post-harvest winter season (median = $7\text{ ng m}^{-2}\text{ d}^{-1}$), thus suggestive that winter conditions were more conducive to aqueous MeHg export. This variability suggests that seasonal differences in MeHg transport may be related to storage in soil or vegetation.

This study addressed two major hypotheses:

- 1) Seasonal uptake and storage of THg and MeHg in vegetation influence hydrologic and biotic mercury export from wetland ecosystems.
- 2) Decay of rice residue on surface soils promotes MeHg production by supplying significant pools of microbial carbon and/or Hg.

To address these hypotheses, data were collected across multiple plant species and replicate fields, focusing on plant growth, elemental carbon (C) and nitrogen (N) composition, decomposition, and tissue concentrations (root, leaf and seed) of THg and MeHg, as described below.

2. Site description

The Yolo Bypass Wildlife Area (YBWA) comprises more than 250 ha of mixed-use wetlands for agricultural production and wildlife management. This study was a component of an intensive interdisciplinary study quantifying MeHg production, export, and bioaccumulation for duplicate fields of 5 wetland types over a full crop year (June 2007–May 2008). Seasonal comparisons were made of Hg, C and N concentrations for biomass growing in three types of flooded agricultural wetlands (white rice, wild rice, and fallow fields), and two permanently flooded, non-agricultural managed wetland areas dominated by different species – cattail (*Typha* spp.) and hardstem bulrush, a.k.a. tule (*Schoenoplectus acutus*; Table 1). Replicate field sites were distributed between northern and southern blocks of YBWA, in which water source and recirculation patterns were slightly different, as described by Windham-Myers et al. (this issue-a). Location, management and seasonal conditions varied among the fields, and are summarized by field in the project synthesis by Windham-Myers et al. (this issue-a). Fields were hydrologically managed for specific vegetation cover, as described in Table 1.

3. Methods

3.1. Seasonal biomass pools and fluxes

Plant tissue samples (leaf, root, seed, litter), aboveground and belowground distribution of biomass, and leaf area were measured in order to assess their physical and biogeochemical influences on Hg cycling, as well as associated C and N standing stocks. Vegetation sampling was concurrent with sediment sampling (Marvin-DiPasquale et al., this issue). Seeds were collected in late August from wild rice and white rice, and again in early December along with cattail and tule seeds in the permanently flooded wetland. Immature rice seeds from the August sampling were compared with abandoned seed heads of white rice collected in early December to determine whether rice seed concentrations were altered by the time of winter flooding when habitat use by overwintering waterfowl is greatest. Harvested rice yield was estimated by field using processed rice dry weight data from the farmer (Table 1).

Live belowground biomass was characterized for the dominant species in each field during all five sampling events (June, July, August, and December 2007, and February 2008), as total live biomass to 30 cm depth (g m^{-2}), live root depth, and live root density in surface soils (0–2 cm). Samples were collected from triplicate plots in each of 9 wetlands ($n = 6$ agricultural and $n = 3$ nonagricultural). Biomass generally was represented by a single dominant species in each field, except for the vegetated fallow field (F66), which was dominated by *Cyperus difformis* (umbrella sedge) but contained additional weed species, especially *Echinochloa oryzoides* (early water grass), *Sagittaria longiloba* (arrowhead), *Typha* spp. (cattail), and *Heteranthera limosa* (ducksalad).

Live aboveground biomass was present in permanent wetlands at all 5 sampling time points, but only in July–August in wild rice fields (W32 and W6), July–August in the one vegetated fallow field (F64), and July–September for white rice fields (R31 and R64). When present, live aboveground biomass (g m^{-2}) was collected by harvesting of 0.25 m^{-2}

Table 1

Field descriptions of dominant plant species, seasonal management events and yield during the 2007–2008 study period. Key characteristics of plant community structure during summer growing season for crops and extant vegetation in each field and during winter in permanent wetland. Field type designations: Ag, agricultural (rice production); non-Ag, non-agricultural (managed wetland for wildlife). Notations: kg ha⁻¹, kilogram per hectare; NA, not applicable.

Field properties					Management			Hydrology				Crop
Field type	Field description	Field code	Block	Dominant plant (genus species varietal)	Tilling	Fertilizer	Pesticide	Crop floodup	Crop drawdown	Winter floodup	Spring drawdown	Rice yield (kg ha ⁻¹)
Ag	White rice	R31	N	<i>Oryza sativa</i> S-102	May	June, July	June, July	June	October	December	March	1272
Ag	White rice	R64	S	<i>Oryza sativa</i> Akita	May	June, July	June, July	June	October	December	March	704
Ag	Wild rice	W32	N	<i>Zizania palustris</i> – Franklin	May	June, July	NA	June	September	December	March	253
Ag	Wild rice	W65	S	<i>Zizania palustris</i> – Franklin	May	June, July	NA	June	September	December	March	226
Ag	Fallow	F20	N	Barren	June	NA	NA	July	August	December	March	NA
Ag	Fallow	F66	S	Mixed – <i>Cyperus difformis</i>	June	NA	NA	July	August	December	March	NA
Non-Ag	Permanent wetland	PW-Cat	S	<i>Typha</i> spp. (Cattail)	NA	NA	NA	NA	NA	NA	NA	NA
Non-Ag	Permanent wetland	PW-tule	S	<i>Schoenoplectus acutus</i> (tule)	NA	NA	NA	NA	NA	NA	NA	NA

quadrants ($n = 3$ per field). Tissues were bagged separately, refrigerated and returned to the laboratory for subsampling within 72 h of collection. Samples were separated into leaf and stem tissue, rinsed of surface debris with deionized water, air-dried, and weighed with a handheld, 1-kg pesola scale. Subsamples of leaf and stem tissues ($n = 5$ for each species) were then oven-dried to constant weight (70 °C for ~48–72 h) to determine an oven-dried: air-dried conversion factor.

Root biomass, root (% volume of surface soils), and depth profiles were determined based on 30 cm deep cores ($n = 2$ per field). Within 72 h of collection, the cores were cut into 2 cm depth intervals in the laboratory. Live roots were manually harvested with forceps and rinsed of soil particles, then visually identified by turgidity and color. A subsample of live root material was subjected to a vital stain (1% tetrazolium red) followed by dissection under 40× magnification, to assess errors of commission (<5% for all samples collected). These samples were then freeze-dried and weighed to assess root biomass (dry weight) at each depth. Three additional surface sediment cores were collected at each site for analysis of root biomass and root density in the 0–2 cm depth interval, along with sediment chemistry and physical characteristics as listed in Windham-Myers et al. (this issue-b). In each replicate surface sediment core, live roots were thoroughly rinsed and then assessed for volume by displacement of deionized water in a 50 or 100 ml graduated cylinder. To verify the different approaches, root biomass values from the 0 to 2 cm interval and from the 0 to 30 cm deep root profiles were compared. In all cases, the root biomass from the 0 to 2 cm surface interval was found to be similar to the biomass calculated using the deeper surface sediment cores (within ± 1 standard error).

3.2. Seasonal biomass elemental tissue composition and storage

For elemental C and N analyses of live tissues (July, August, and December 2007), samples of fresh leaf, root, and seed tissues (50–100 g wet weight) from a single species (see Table 1) were subsampled in triplicate plots within each field. Approximately 50 g were refrigerated until further processing, and ~20–50 g were flash-frozen on dry ice immediately for Hg and MeHg analyses. Within 72 h of collection, refrigerated leaf surfaces and live root tissues were rinsed with deionized water and a 1% EDTA solution to remove adsorbed THg and other particulates. All samples (both washed samples and field-frozen samples) were then freeze-dried, ground and homogenized in a polycarbonate vial with silica beads (0.3 mm diam, Cole Parmer Laboratory Jar Mill). Surficial contamination appeared to be minimal, as no consistent differences were observed in Hg and MeHg concentrations between tissues of each preparation.

Tissue concentrations of carbon (C) and nitrogen (N) were measured using a Carlo-Erba NC-2500 elemental analyzer interfaced to a Micromass Optima mass spectrometer operated in continuous flow mode. Leaf tissues collected during August 2007 were further assayed for lignin concentration using acetyl-bromide extraction and

spectrometry (Iiyama and Wallis, 1988). Tissue THg concentrations were analyzed using a microwave-assisted nitric acid (HNO₃) digestion followed by Hg analysis on a Tekran 2600 automated CVAFS unit, according to a modified version of EPA 1630 (DeWild et al., 2004). MeHg concentrations were measured following extraction with KOH: methanol, ethylation, and fluorescence spectroscopy (CVAFS), as per Marvin-DiPasquale et al., this issue). A subset of samples were also assayed for sediment contamination by mineral content (via combustion and calculated loss on ignition), and aluminum (Al) or titanium (Ti) content (via ICP-AES). Quality assurance for trace metal analyses was met with laboratory duplicates (RSD = 2% \pm 2% for MeHg, 20% \pm 2% for THg), recovery of trace elements in reference materials (IAEA 140/TM, *Fucus* spp; 96% \pm 6% for THg, 98% \pm 5% for MeHg; SRM 1547 Peach Leaf, Al: 98% \pm 1%, Ti: 99% \pm 2%), and matrix spike recoveries (QA = 90% \pm 5%; for MeHg, 96% \pm 1% for THg).

3.3. Surface litter production and decomposition

Aboveground biomass (by dry weight) was assessed in June, July, August, and December 2007 with harvest of replicate plots in the 5 vegetated agricultural fields and the 2 non-agricultural, permanent wetlands ($n = 7$ tissue types). Photosynthetic leaf tissues represented 58 to 95% of aboveground biomass for all crop and weed species. August estimates of total aboveground biomass were used as initial estimates of litter abundance. The rate of decomposition of aboveground tissues was assayed by a laboratory experiment that tracked particulate and dissolved pools of carbon and Hg from tissues under submerged aerobic conditions (e.g. Devevre and Horwath, 2000). Carbon (C) mineralization, DOC release, and dissolved THg release during tissue decomposition were assayed on August 2007 leaf samples from the six agricultural fields and the two permanent wetland communities. Leaves were first rinsed briefly in a 1% EDTA solution, followed by deionized water and blotted dry. Prior to incubation, tissues were freeze-dried and pulverized to homogenize tissues between replicates, as well as to focus the experiment on the biochemical rather than on the structural differences between leaf tissues. Leaf tissues from all fields were assayed for daily decay rate constants (k_{decomp}), except from the barren fallow field (F20) which lacked consistent plant cover. For the latter, a single dominant species – *C. difformis* (sedge) – was chosen from the vegetated fallow field (F66).

For each of the seven treatments ($n = 5$ agricultural and $n = 2$ non-agricultural), 4.8 to 5.2 g of prepared leaf tissues were added to replicate ($n = 5$) combusted Pyrex glass centrifuge tubes (50 ml), with five centrifuge tubes for control incubations (no leaf material added). A 40 ml aliquot of deionized water (Ultrapur MQ) was added to each of the 40 vials, representing 8 treatments in all (7 field treatments + 1 control [no leaf tissue]). To ensure maximum decomposition rates and compare with literature estimates for rice residue decay (Devevre and Horwath, 2000), vials were incubated at 30 °C for 28 days under oxic conditions and constant gentle

agitation (50 rpm on a shaker table). A foam plug was inserted into the top of each vial to allow for gas exchange with the atmosphere, while minimizing the loss of water due to evaporation. All vials were tested weekly for the presence of sulfide using an ion-specific electrode (Cole Parmer ISE 27502) and for dissolved oxygen (D.O.) concentrations (Hanna Instruments 9142) on Day 28, at which time all were > 10% D.O. saturation. The incubation water was monitored for volume each week and used to correct for total mass of solution. Volume loss to evaporation was recorded to the nearest ml, and represented approximately 2 to 3 ml per week. Subsamples (5 ml) were collected (and replaced with deionized water) at five time-points from each vial (day 0, 1, 7, 14 and 28) and prepared for analysis of aqueous THg, DOC, and particulate matter. On Day 28, the final collections of THg and C pools (dissolved and particulate) were made using the entire 40 ml of solution. THg concentrations in the initial incubation water were less than 0.2 ng L^{-1} , and control vial THg concentrations remained within 25% relative standard deviation (RSD) of this initial concentration throughout the experiment.

Upon retrieval, the contents were filtered through combusted pre-weighed GFF filters (0.7 μm nominal poresize), to determine the remaining particulate mass (detritus) GFF filters. Approximately 1 ml of filtrate was subsampled and assayed for DOC concentrations on a Shimadzu TOC 5000a analyzer. The remaining filtrate (~39 ml) was returned to the centrifuge tube and 200 μl of BrCl (0.5% v/v) was added to preserve and extract any Hg that may have adsorbed to the vial walls. This incubation filtrate was then filtered at 0.45 μm (nylon filters) and transferred to Teflon bombs, for processing and analysis of for total Hg concentration by CVAFS according to EPA 1631 (U.S. EPA 2002).

Plant tissue mass loss was calculated as the initial tissue mass minus the final particulate material mass in each vial, corrected for dry weight. Tissue C loss was thus estimated as a function of both DOC release and oxidation (gaseous carbon loss), by correcting mass for tissue %C. The particulate remaining on filters was combusted to determine the organic content. Differences in particulate matter from Day 1 to Day 28 were used to calculate a logarithmic decay rate (k_{decomp}) based on laboratory conditions.

To estimate decay rates under flooded field conditions across the seasonal temperature gradient, laboratory measurements were scaled according to a Q_{10} of 2.44 (Gu et al., 2004), on monthly time-steps of average monthly temperatures as recorded by California Department of Fish and Game at El Macero Station (Yolo Bypass). Posthoc validation of this Q_{10} for litter decay included published data on flooded rice decay (Devevre and Horwath, 2000; Bird et al., 2003) and coordinated measurements of sulfate reduction rates in the openwater sites (PW5-OW) across seasons (the only site where %OM did not vary seasonally) yielded an composite Q_{10} of 2.50 (temperature ranged from 9 to 23 °C; see Marvin-DiPasquale et al., this issue). These rates were then combined with initial biomass pools (aboveground biomass in August), and the date of litter deposition (harvest date or for fallow fields, the draw-down date) to estimate the pool size of surface detritus through time within each field type. These estimated pools of surface litter were compared with surface measurements of litter pools in February 2008. The patchy distribution and sediment content of the surface litter made for highly variable and unreliable weight estimates of field-borne detrital mass from field replicates (RSD > 100%, unpublished data). Thus, we compare predicted pools of surface detritus rather than field-borne pools of detritus, as they showed similar patterns among wetland types (e.g. Rice > WildRice > Fallow) but were more consistent in representing seasonal rice residue (Bird et al., 2003), as well as C and Hg turnover.

The rate constant associated with tissue decomposition (k_{decomp}) was compared between tissue types by MANOVA using time (0–28 days) as a continuous covariate. Carbon loss that could not be accounted for in DOC pools after 28 days of incubation was assumed to be indicative of complete C respiration to CO_2 . The total Hg released during decomposition

was assessed between tissue types for the difference between the initial and final subsample (Day 0 and Day 28).

3.4. Biotic exposure and transport by seed consumption

We calculated the potential biotic ingestion of THg and MeHg in waterfowl in the Central Valley of California, using the following formula:

$$\text{Hg (ng/day)} = \left(\frac{\text{DEE (kJ/day)}}{\text{TME (kJ/g dw)}} \right) \times (\text{seed Hg (ng/g dw)})$$

where DEE is the daily existence energy required for waterfowl (kJ/day), TME is the true metabolizable energy of a given seed type for waterfowl (kJ/g dw), and seed Hg is either the total or methyl mercury concentration of a husked seed. Daily existence energy of a free-living waterfowl was estimated to be 4 times the resting metabolic rate of waterfowl (following a review by Heitmeyer, 2010), rather than 3 times resting metabolic rate as was used by Miller and Eadie (2006), to incorporate costs of daily activities such as flight and foraging. Following Miller and Eadie (2006), we used 512 (kJ/day) as the resting metabolic rate of the average waterfowl present (weight of 1.3 kg) in the Central Valley of California during the winter. The daily existence energy divided by the true metabolizable energy of a given seed type yields the amount of food of that seed type (g dw) required to be consumed per day on average to maintain body condition (Miller and Eadie, 2006; Heitmeyer, 2010). We used 13.98 kJ/g (Reinecke et al., 1989), 14.52 kJ/g (Sherfy, 1999), and 10.46 kJ/g (Reinecke et al., 1989; Checkett et al., 2002) as the value for true metabolizable energy of white rice, wild rice, and moist-soil seeds, respectively, for waterfowl. We converted kcal to kJ assuming $\text{kJ} = 4.185 \times \text{kcal}$ (Gabrielsen et al., 1991). We then multiplied the amount of food required per day by the Hg concentration of that food (this study) to estimate the amount of Hg exposure per day. We recognize that ingestion does not directly relate to bioaccumulation, and focus here only on dietary biotic exposure.

3.5. Statistical analyses

Statistical analyses were performed using Spotfire SPlus 8.1 (TIBCO, 2008). Data from the 7 ($n = 5$ agricultural and $n = 2$ non-agricultural) vegetated sites were assessed for comparisons between fields at peak biomass and for comparisons among months (July, August, and December) for seasonal trends. Normality of each parameter was assessed with Kolmogorov–Smirnov tests, and non-normal data were log-transformed. Means and standard deviations are reported for seasonal and spatial comparisons. Data were assessed for significance ($p < 0.05$) between discrete field types and seasons using a mixed-effect ANOVA with field-ID as a random effect. Data were also analyzed for block effects (northern versus southern field replicates), but none were found across all parameters measured. Pearson correlation analysis of parameters within given field types are only reported where significant ($p < 0.05$), by comparison with t_{crit} for a two-tailed distribution and $df = 1$. Linear or logarithmic regressions are reported for predictive relationships with $p < 0.05$.

4. Results

4.1. Seasonal biomass pools and fluxes

Vegetative growth was rapid in the agricultural fields (Fig. 1). Over 76 days, between June and August sampling events, white rice fields generated $2.1 \pm 0.2 \text{ kg}_{\text{dw}} \text{ m}^{-2}$ of total biomass (above- and belowground; average of fields R31 and R64). Over the same interval, wild rice fields generated $1.5 \pm 0.3 \text{ kg}_{\text{dw}} \text{ m}^{-2}$ of biomass (average of fields W32 and W65). At roughly $24 \pm 4 \text{ g}_{\text{dw}} \text{ m}^{-2} \text{ d}^{-1}$ these rates are consistent with global ranges of rice crop growth (Mitsch et al.,

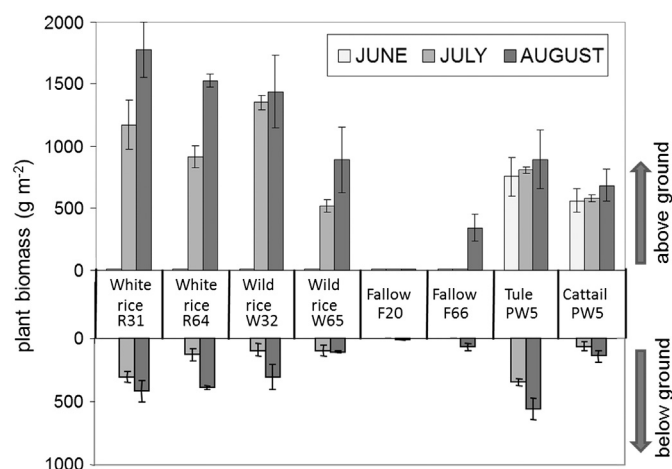


Fig. 1. Bar graph of above and below-ground plant biomass in each field during the summer growing season, June–August 2007. Plant biomass is given on a dry weight basis. Error bars denote ± 1 standard deviation ($n = 3$).

2010), and approximately twice as great as the weed productivity in the fallow agricultural fields ($0.4 \pm 0.1 \text{ kg}_{\text{dw}} \text{ m}^{-2}$ over 31 days, or $\sim 12 \text{ g}_{\text{dw}} \text{ m}^{-2} \text{ d}^{-1}$). The use of fertilizer, flow through irrigation, and herbicide (in the white rice) (Table 1; also see Bachand et al., this issue-b) are likely to explain the comparatively high productivity of white rice and wild rice relative to fallow fields.

After seeding in June 2007, white rice and wild rice phenology were at a pre-heading (early panicle development) condition in July 2007, and post-heading condition in August 2007. In July 2007, leaf biomass dominated the aboveground biomass component, representing more than 82% of the biomass in all samples collected. Allocation to stem tissue increased slightly during the heading phase, such that leaf tissue represented 58 to >95% of aboveground biomass in August 2007. Root biomass was fairly consistent in July and August, but varied strongly between wetland types (Table 2) ranging from $563 \text{ g}_{\text{dw}} \text{ m}^{-2}$ in tule stands in the permanent wetland to $74 \text{ g}_{\text{dw}} \text{ m}^{-2}$ in fallow field F66 (Table 3). Belowground biomass represented $\leq 20\%$ of total biomass in white rice fields, $\leq 10\%$ of total biomass in wild rice fields, and 35% of total biomass in the permanent wetland tule stand. Thus, aboveground biomass dominated the total vegetative biomass pools, such that ratios

of above:belowground biomass ranged from 2 to 12, and were not significantly different among seasons ($F_{2,24} = 1.33$, $p = 0.3715$).

Permanent wetland vegetation biomass did not differ from agricultural vegetation at peak biomass (Table 2), but had a much longer growing season. Patterns for standing live aboveground biomass (g m^{-2}) in tule and cattail communities were similar, at consistently high values from June to December ($1.2 \pm 0.3 \text{ kg}_{\text{dw}} \text{ m}^{-2}$). Total root biomass also did not change significantly with season in permanent wetland plots dominated by these perennial emergent macrophytes (Table 2). Thus, in contrast to the agricultural fields, rates of net primary productivity were spread through the year in permanent wetlands, and during summer months, vegetation did not gain significant live biomass, likely due to earlier spring growth and the high cost of respiration in the deeply anoxic sediment (e.g. Grace and Wetzel, 1998; Rocha et al., 2008), as well as due to relatively lower availability of nutrients as compared with fertilized fields.

Root biomass was heavily concentrated in the upper 0 to 2 cm of the root profile at all sites and in all seasons ($74\text{--}302 \text{ g m}^{-2}$; 32 to 100% of total root biomass). Surface root biomass and root density (% volume of root biomass per volume of soil) were strongly correlated among all fields in July and August 2007 ($r = 0.89$). Density of live roots in surface sediment reached a seasonal maximum within agricultural fields during July and August, but did not vary seasonally in the permanent wetland sites (Table 2).

Seed biomass represented only a small fraction (<3%) of total net primary productivity in all fields in summer, from ~ 35 to $63 \text{ g}_{\text{dw}} \text{ m}^{-2}$ in white rice fields in September, to ~ 11 to $13 \text{ g}_{\text{dw}} \text{ m}^{-2}$ in wild rice fields in August (Table 3), but harvest yields were greater once the grains had matured (Table 1).

4.2. Seasonal biomass elemental tissue composition and storage

The most significant differences in tissue quality parameters were found between field type, and not between blocks or among seasons (Table 3). Leaf tissues showed higher concentrations of N than root tissues at peak biomass (Table 3), and throughout the growing season. Among fields managed for agriculture, tissue N concentrations varied strongly between species, with the highest leaf N concentrations observed in fallow field weeds (2.9%), followed by white rice ($1.4 \pm 0.4\%$), and then by wild rice ($0.5 \pm 0.1\%$). Tissue N concentration differences resulted in over a 3-fold range in carbon:nitrogen (C:N) ratios between the two crops, white rice (28 ± 11) and wild rice (92 ± 21), and

Table 2

Mixed effect analysis of variance (ANOVA) for vegetation metrics, based on month ($n = 3$) and vegetation types ($n = 5$, white rice, wild rice, fallow, and permanent wetland cattail and tule), with field ID as a random effect. For biomass and root density data, seven sites were compared instead of eight as F20 was excluded due to lack of rooted vegetation in the sampling region. Seed MeHg concentration was compared for 6 fields, and lacked a balanced seasonal comparison. Three months are compared – July (pre-heading), August (post-heading), and December.

	Month		Type		Month * type		ID within type	
	df	Fvalue	df	Fvalue	df	Fvalue	df	Fvalue
Aboveground biomass	2	9.56****	3	59.7****	3	0.867 ^{NS}	4	5.79***
Belowground biomass	2	1.44 ^{NS}	3	11.1****	3	0.978 ^{NS}	4	5.55**
Surface root density (0–2 cm)	2	1.41 ^{NS}	3	8.4***	3	1.12 ^{NS}	4	6.1***
Biomass Hg pool	1	0.503 ^{NS}	3	6.66**	2	4.80*	4	2.64 ^{NS}
Biomass MeHg pool	1	12.7**	3	1.47 ^{NS}	2	13.2****	4	2.69*
Root Hg concentration	1	1.19 ^{NS}	3	6.45**	2	1.92 ^{NS}	4	1.41 ^{NS}
Leaf Hg concentration	1	22.7****	3	9.97****	2	73.8****	4	0.74 ^{NS}
Seed Hg concentration	NA		2	287****	NA		3	13.8***
Root MeHg concentration	1	17.8***	3	35.8****	2	12.7****	4	1.57 ^{NS}
Leaf MeHg concentration	1	2.21 ^{NS}	3	5.04**	2	90.0****	4	0.343 ^{NS}
Seed MeHg concentration	NA		2	41.7****	NA		3	0.216 ^{NS}

NA = not applicable.

NS = not significant.

* p value < 0.05.

** p value < 0.01.

*** p value < 0.001.

**** p value < 0.0001.

Table 3

Concentrations of carbon, nitrogen, mercury, and methylmercury and biomass of plant tissue in individual fields in August 2007. Means and standard deviations (reported in parentheses) represent a minimum of $n = 3$ field samples. All pools and concentrations for individual tissues are provided on a dry weight basis. Ratios of C:N and MeHg:THg in plant tissues are calculated from mean concentrations. No assessment of these parameters was made for vegetation associated with the seasonal wetland site. C, carbon; N, nitrogen; %, percent; THg, total mercury; MeHg, methylmercury; ng g^{-1} , nanogram per gram; g m^{-2} , gram per square meter; $\mu\text{g m}^{-2}$, microgram per square meter; ND, not determined.

Field code	Dominant plant type	Plant biomass (g m^{-2})	Carbon (%)	Nitrogen (%)	C:N ratio	THg (ng g^{-1})	MeHg (ng g^{-1})	MeHg/THg ratio	Carbon (g m^{-2})	Nitrogen (g m^{-2})	THg ($\mu\text{g m}^{-2}$)	MeHg ($\mu\text{g m}^{-2}$)
<i>Leaf data</i>												
R31	White rice	1139 (27)	36.9 (1.2)	1.8 (0.6)	20	14 (4)	2.6 (0.2)	19%	420 (12)	20.7 (3.7)	16 (2)	3.0 (0.1)
R64	White rice	984 (12)	36.7 (0.8)	1.0 (0.2)	37	15 (9)	1.3 (0.4)	9%	361 (6)	9.8 (1.0)	15 (5)	1.3 (0.2)
W32	Wild rice	1027 (10)	40.4 (1.1)	0.4 (0.1)	107	107 (11)	4.4 (0.5)	4%	415 (8)	3.9 (0.5)	110 (6)	4.5 (0.3)
W65	Wild rice	942 (30)	38.6 (2.4)	0.5 (0.1)	77	101 (8)	1.7 (0.1)	2%	364 (17)	4.7 (0.5)	95 (5)	1.6 (0.1)
F20	Plantain/algae	10 (9)	40.6 (0.1)	2.9 (0.4)	14	37 (4)	3.1 (0.9)	8%	4.1 (1.8)	0.3 (0.2)	0.4 (0.2)	0.03 (0.02)
F66	Sedge	330 (34)	34.5 (1.1)	1.7 (0.2)	20	31 (5)	5.6 (0.4)	18%	114 (8)	5.6 (0.6)	10 (1)	1.8 (0.2)
PW5	Tule	1404 (50)	41.0 (1.8)	0.7 (0.0)	59	50 (6)	0.5 (0.1)	1%	576 (23)	9.8 (0.2)	70 (5)	0.7 (0.1)
PW5	Cattail	1188 (36)	40.3 (2.2)	0.8 (0.1)	50	55 (11)	0.4 (0.1)	1%	479 (18)	9.5 (11)	65 (4)	0.5 (0.1)
<i>Root data</i>												
R31	White rice	424 (83)	12.2 (0.2)	0.7 (0.2)	17	273 (25)	3.1 (2.4)	1%	52 (5)	3.0 (0.7)	116 (17)	1.3 (0.6)
R64	White rice	395 (19)	16.7 (0.2)	0.8 (0.1)	21	295 (36)	10.2 (2.1)	3%	66 (2)	3.2 (0.2)	117 (10)	4.0 (0.5)
W32	Wild rice	308 (101)	32.6 (0.8)	0.7 (0.0)	47	279 (22)	12.4 (1.9)	4%	100 (18)	2.2 (0.4)	86 (17)	3.8 (0.9)
W65	Wild rice	107 (12)	28.3 (0.1)	0.5 (0.0)	57	105 (41)	10.9 (2.5)	10%	30 (2)	0.5 (0.0)	11 (3)	1.2 (0.2)
F20	Plantain/algae	1.0 (3.0)	22.4 (0.2)	1.0 (0.0)	22	214 (77)	12.3 (1.1)	6%	0.2 (0.3)	0.01 (0.02)	0.2 (0.4)	0.01 (0.02)
F66	Sedge	74 (27)	27.6 (0.1)	0.9 (0.0)	31	247 (12)	10.6 (0.4)	4%	20 (4)	0.7 (0.1)	18 (4)	0.8 (0.2)
PW5	Tule	563 (88)	36.3 (0.1)	1.4 (0.0)	26	150 (26)	1.2 (0.6)	1%	204 (16)	7.9 (0.6)	84 (14)	0.7 (0.2)
PW5	Cattail	143 (49)	38.3 (0.2)	1.2 (0.0)	32	104 (18)	1.9 (0.8)	2%	55 (10)	1.7 (0.3)	15 (4)	0.3 (0.1)
<i>Seed data</i>												
R31	White rice	28 (13)	41.5 (0.2)	1.6 (0.1)	26	54 (12)	4.1 (1.1)	8%	6.6 (2.3)	0.3 (0.1)	0.9 (0.4)	0.1 (0.0)
R64	White rice	16 (11)	39.4 (0.1)	1.2 (0.3)	33	46 (6)	4.2 (0.6)	9%	11 (3)	0.3 (0.1)	1.3 (0.4)	0.1 (0.0)
W32	Wild rice	12 (6)	44.1 (2.1)	1.6 (0.1)	28	11 (2)	6.6 (1.4)	60%	5.3 (1.4)	0.2 (0.1)	0.1 (0.0)	0.1 (0.0)
W65	Wild rice	10 (8)	42.5 (0.1)	2.3 (0.2)	18	16 (12)	5.9 (1.6)	37%	4.3 (1.7)	0.2 (0.1)	0.2 (0.1)	0.1 (0.0)
F20	Plantain/algae	0 (0)	ND	ND	ND	ND	ND	ND	ND	ND	ND	ND
F66	Sedge	0 (0)	ND	ND	ND	ND	ND	ND	ND	ND	ND	ND
PW5	Tule	4 (9)	41.0 (0.1)	1.1 (0.1)	37	150 (26)	1.2 (0.2)	1%	1.6 (1.8)	0.04 (0.05)	0.6 (0.7)	0.005 (0.006)
PW5	Cattail	21 (15)	44.2 (0.5)	1.0 (0.1)	44	104 (18)	1 (0.4)	1%	9.3 (3.4)	0.2 (0.1)	2.2 (1.0)	0.02 (0.01)

over a 4-fold variation in aboveground biomass N pools between white rice ($18 \pm 4 \text{ g m}^{-2}$) and wild rice ($4 \pm 1 \text{ g m}^{-2}$). The dominant fallow field weed (sedge, *C. difformis*) was similar to the average white rice C:N ratio (20 ± 3), but the low biomass yielded a low pool of N in vegetation for (field F66 = $5.6 \pm 0.6 \text{ g N m}^{-2}$). The leaf tissue C:N ratios of cattail (59 ± 23) and tule (50 ± 14) were similar, but tended to be lower than the wild rice C:N ratios. Another notable difference by species was the high ash content (loss on ignition, LOI) in white rice and wild rice (up to 4% of leaf tissue composition). Elemental analysis by ICP-AES further suggested that silica comprised the majority of this mineral component in all species (900–16,200 ppm). Although ash, silica or %C contents were variable and not significantly different between species, %LOI and %C were positively correlated ($R = 0.86$, $p < 0.05$), suggesting that the mineral or ash component plays a direct role in diluting carbon pools in standing stock biomass and later during litter decay on the sediment surface. Lignin concentrations were significantly greater in tule and cattail (3.1–22%) leaves than in white rice, wild rice, or fallow weed leaves (0.2–2.4%; one-way ANOVA, $F_{4,28} = 174.01$, $p < 0.0001$).

Plant tissue THg pools and concentrations in August also varied significantly by species, but not between blocks ($p > 0.05$, Fig. 2a; Table 3). Total Hg concentrations were greatest in roots, with mean values ranging from 104 ng g^{-1} in cattail roots to 282 ng g^{-1} in white rice roots. Total Hg concentration in root tissues was not predicted by sediment THg concentrations even when constrained to annual agricultural species only, likely due to the limited range of sediment THg variability observed among the agricultural soils (Mean and SD = $333 \pm 45 \text{ ng g}_{\text{dw}}^{-1}$). Root sample concentrations of Al (<10 ppm) and Ti (<5 ppm) illustrated that soil contamination represented less than 0.1% of the root sample by weight and thus cannot account for the high THg concentrations. No differences were observed among species or fields in agricultural wetlands, but all agricultural wetlands had higher root THg concentrations than non-agricultural wetlands

(Tables 2 and 3). Because permanent wetlands were concentrated on the eastern edge of the Yolo Bypass, we note that the doubling of surface sediment THg concentrations along an east–west gradient may play a role in root THg concentrations (see Marvin-DiPasquale et al., this issue).

In contrast, leaf concentrations varied by almost 1 order of magnitude among species, with leaf THg concentrations of $104 \pm 8 \text{ ng g}^{-1}$ in wild rice leaves and $14 \pm 3 \text{ ng g}^{-1}$ in white rice leaves (one-way ANOVA, $F_{3,24} = 124.0$, $p < 0.0001$). Non-crop species (sedge, tule, and cattails) all showed similar leaf tissue concentrations, ranging from 30 to 55 ng g^{-1} . The low THg concentration in white rice leaf tissue was notable, considering the species had among the highest mean THg concentrations in plant roots (284 ng g^{-1}). Further, there was greater than a 6-fold difference in THg pools associated with leaf tissue biomass between white rice and wild rice fields ($15 \mu\text{g m}^{-2}$ and $100 \mu\text{g m}^{-2}$, respectively). Ratios of C:N for leaf tissues were significantly correlated with THg concentrations ($r^2 = 0.86$), such that THg was inversely associated with N concentrations. Stoichiometrically, this suggests significant physiological and biochemical differences between these plant species in uptake pathways (e.g. Stein et al., 1996), root:shoot translocation rates (e.g. Schwesig and Krebs, 2003), and/or sulfhydryl binding sites (e.g. Patty et al., 2009), but these were not directly assessed in this study.

In contrast to the leaf THg concentrations, seed THg concentrations were significantly greater in white rice than wild rice ($50 \text{ v } 13 \text{ ng g}_{\text{dw}}^{-1}$), with high concentrations in the wild rice husk (up to $95 \text{ ng g}_{\text{dw}}^{-1}$). Husk removal was not attempted for white rice, and thus the differences in seed concentrations may partially reflect structural differences between white and wild rice in husk characteristics. More importantly, these data suggest that tissue level differences are not constant across entire plants and may indicate varied physiologic processes of uptake, translocation, and storage.

Despite large seasonal differences in soil MeHg concentrations (Marvin-DiPasquale et al., this issue), MeHg concentrations in roots

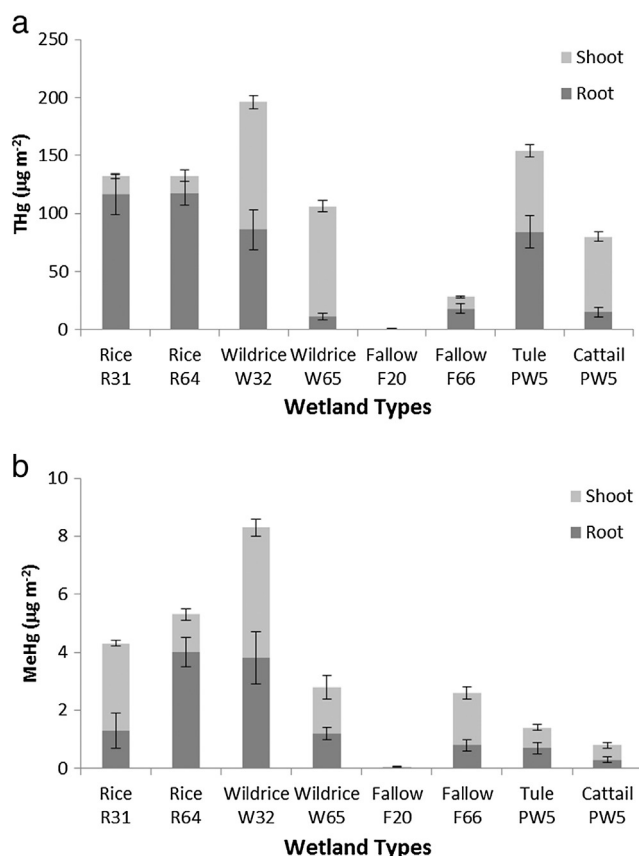


Fig. 2. a–b. Bar graph of above and below-ground (shoot and root) plant mercury pools in each field in August 2007, for a) total mercury, and b) methylmercury in $\mu\text{g m}^{-2}$. Error bars denote ± 1 standard deviation compounded for biomass and concentration data ($n = 3$).

and leaves remained similar from July through December, suggesting uptake commensurate with growth (Table 2). Among agricultural fields, August concentrations of MeHg were similar among fields within a given tissue type, and much larger than tissue concentrations in permanent wetland species (Table 3). Tule and cattail had 3- to 8-fold lower MeHg concentrations in their leaves (0.5 ng g^{-1}), ~8-fold lower MeHg concentrations in their roots (1.6 ng g^{-1}), and ~4-fold MeHg lower concentrations in their seeds (1.1 ng g^{-1}). MeHg concentrations in tissues were not correlated with THg concentrations and in many cases showed opposite patterns. While MeHg represented 8 to 9% of the THg pool in white rice seeds, MeHg constituted 37 to 60% of the THg pool in wild rice seeds (Table 3). No seasonal or block patterns were observed (Table 2), but MeHg concentrations were significantly greater in agricultural tissues than permanent wetland species tissues (Table 2), including roots ($p < 0.0001$), leaves ($p = 0.0004$) and seeds ($p = 0.0032$). MeHg concentrations were greater in whole seeds (unhusked) than in leaves for both rice crops (seeds = $4.2 \pm 1.1 \text{ ng g}^{-1}$ in white rice, $6.2 \pm 1.5 \text{ ng g}^{-1}$ in wild rice), and seed MeHg concentration was better correlated with root MeHg concentration ($r = 0.90$ $p < 0.05$) compared to leaf MeHg concentration ($r = 0.61$ $p < 0.05$). A separate analysis of MeHg in seed husks for wild rice showed the highest concentration of all tissues (up to 29 ng g^{-1}), but this portion is usually removed for crop storage and preparation for human consumption. Residual white rice seed from the December sampling was found to have similar MeHg concentrations with white rice seed collected in August ($5.2 \pm 2.1 \text{ ng g}^{-1}$).

Leaf concentrations of MeHg were relatively similar across field sites, and root concentrations were only marginally correlated with leaf concentrations ($r = 0.39$, $p < 0.1$). Whereas tissue MeHg showed

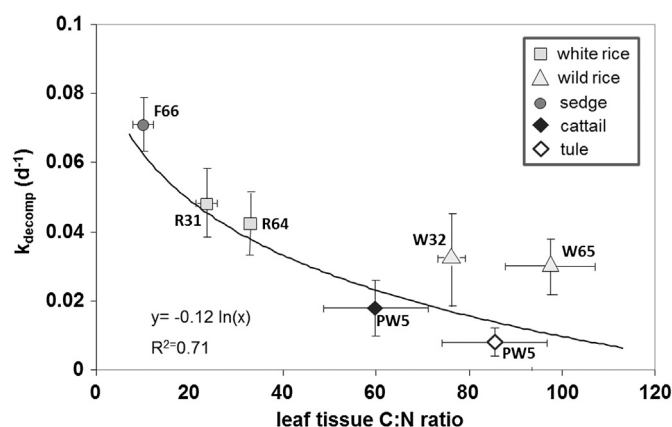


Fig. 3. Scatterplot of leaf tissue carbon-to-nitrogen ratios versus litter decomposition rate constants for the dominant plant species in each field type. Plant tissue decomposition rate constants (k_{decomp}) were assessed experimentally in the laboratory during 28 days of incubations at 30°C . Error bars denote ± 1 standard deviation. An exponential regression was fit to the data ($y = -0.12 \ln(x)$) and was significant at $p = 0.0120$.

some slight increases during the growing season in rice fields, as did sediment MeHg concentrations, MeHg concentrations were not correlated between roots and 0 to 2 cm surface soils for any given sampling event, whether assessed across all wetlands or only agricultural wetlands.

MeHg was abundant in surface soils in all wetlands in August ($> 1 \text{ ng g}^{-1}_{\text{dw}}$; Marvin-DiPasquale et al., this issue) but differences in plant physiologic processes (translocation, rooting depth) may have limited the direct correlation of sediment MeHg production and root MeHg concentration. Both root and leaf MeHg concentrations were not predicted from soil concentrations of MeHg, THg, or the bioavailable or “reactive” fraction of THg (Marvin-DiPasquale et al., this issue). High variability among leaves in MeHg concentrations suggest that leaf age, timing, and growth rate may influence the MeHg load of individual leaves (Weis et al., 2003). Considering compounded errors, peak MeHg pools in vegetation were highly variable within and among wetlands (Fig. 2b). Average daily uptake was relatively small (2 to $51 \text{ ng m}^{-2} \text{ d}^{-1}$) compared with potential MeHg production ($> 1000 \text{ ng m}^{-2} \text{ d}^{-1}$) but MeHg storage in vegetation was at a same order of magnitude as calculated daily hydrologic exports of 3 to $18 \text{ ng m}^{-2} \text{ d}^{-1}$ from agricultural wetlands (Bachand et al., this issue-b), thus serving as a temporary but significant storage term during the growing season.

4.3. Surface litter production and decomposition

Decomposition rates were rapid for white rice, wild rice, and fallow species ($> 4\% \text{ d}^{-1}$), and significantly slower for permanent wetland species tule and cattail ($2\% \text{ d}^{-1}$, Table 3). Log-based calculations of k_{decomp} were similar to published rates (e.g. Devevre and Horwath, 2000), and consistent through the entire incubation except for the initial leaching phase. With 5 to 14% of initial mass lost in the first day of incubation for white rice, wild rice and the fallow species. These plant tissues are highly labile as compared with the more waxy and lignin-rich tissues of tule and cattail ($< 2\%$ mass lost on the first day of incubation). Pre-decomposition loss on ignition showed significant ash contents in wild rice ($1.3 \pm 0.9\%$) and white rice ($1.9 \pm 1.0\%$). Selected elemental analyses of leaf tissues showed high silica concentrations in white rice (16200 ppm) and wild rice (12700 ppm).

Rates of mass loss were clearly a function of tissue quality, specifically C:N ratios ($r^2 = 0.71$, Fig. 3) as per Melillo et al. (1982), and less so a function of lignin concentrations ($r^2 = 0.24$). Regression analysis supports the importance of %N as the primary driver of decay dynamics. Additionally, N uptake by crops was evident in their enriched nitrogen isotope (d^{15}N) composition (Marschner, 1995); further d^{15}N

Table 4
Plant litter decomposition rates and areal pool sizes. Plant litter on the sediment surface from September to February 2008 was calculated based on growing season biomass (field measurements), date of litterfall via harvest (rice crop) or senescence (native wetland plants), and the decomposition rate constants (k_{decomp}) at 30 °C determined in the laboratory for each plant species. The temperature-dependent k value was then adjusted for mean monthly in-field air temperature (in °C) as reported by the Calif. Dept. of Fish and Game at El Macero Station, Calif., and was assumed to follow Q10 kinetics (increasing by a factor of 2.4 for every 10 °C change in temperature, as per Gu et al. (2004) and Devereux and Horwath (2000)). Averages and standard deviations (reported in parentheses) represent a minimum of $n = 3$ field samples. %, degree Celsius; g m^{-2} , gram per square meter, on a dry weight basis.

Field code	Plant species	Decomposition rate constant (k_{decomp}) at 30 °C	Estimated litterfall date	Initial biomass at litterfall	Estimated Surface Litter February 2008		Estimated C released		Estimated Hg released	
					Mean	sd	Mean	sd	Mean	sd
				g m^{-2}	g m^{-2}		g m^{-2}		$\mu\text{g m}^{-2}$	
R31	<i>Oryza sativa</i> – S102	–4.2 (0.8)	10/1/2007	1139	391 (31)		276 (22)		10.5 (0.83)	
R64	<i>Oryza sativa</i> – Akita	–4.7 (1.2)	10/1/2007	984	288 (16)		255 (14)		10.4 (0.58)	
W32	<i>Zizania palustris</i>	–2.3 (1.6)	9/1/2007	1027	253 (14)		313 (17)		82.8 (4.58)	
W65	<i>Zizania palustris</i>	–2.8 (0.8)	9/1/2007	942	163 (17)		301 (31)		78.7 (8.21)	
R66	<i>Cyperus difformis</i>	–7.1 (1.0)	10/1/2007	330	18 (2)		108 (12)		9.7 (1.07)	
PW5	<i>Schoenolobos acutus</i>	–2.2 (0.5)	12/15/2007	1404	952* (72)		185 (14)		22.6 (1.71)	
PW5	<i>Typha</i> spp.	–2 (0.8)	12/15/2007	1188	836* (109)		142 (18)		19.4 (2.52)	

* Estimated surface litter for permanent wetland species may include standing dead material, as deposition is episodic and primarily wind-driven.

values of agricultural leaf tissues in August were 2–6 per mil enriched over the fertilizers applied (Alpers et al., this issue). This suggests significant rates of denitrification of fertilizer within the fields, a further indicator of the importance of soil anaerobic microbial processes (Bird et al., 2003).

When scaled to field conditions, estimates of surface litter areal mass remaining was highest in white rice fields and lowest in fallow fields (Table 4). These patterns were found to be correlated with pw[Ac] ($r = 0.71$) an important index of labile carbon supply. Further, estimates of total litter mass in fields present in February 2008 were correlated with calculated rates of k_{meth} ($r = 0.68$). Thus, the role of labile carbon as a driver of Hg(II)-methylating bacteria activity was particularly apparent during February 2008, the period during which the decay of rice straw was being actively facilitated with managed reflooding of the previously harvested rice fields and when the strongest relationship between pw[Ac] and k_{meth} was seen (Fig. 4; Marvin-DiPasquale et al., this issue). Further, the terrestrial signal associated with the characterization of surface water DOC quality (e.g. Emission–Excitation Matrices, EEMs) was correlated with estimates of surface litter areal mass (J.A. Fleck et al., in press).

During vegetative senescence in winter months, live root biomass was present in small quantities but not correlated with MeHg production or concentration. Instead, estimates of surface detritus was a better predictor of pw[Ac] concentrations (labile carbon), k_{meth} , and the relative terrestrial signature of DOC in surface water (an index of fresh carbon supply; Fleck et al., in press), suggesting that MeHg production is carbon-limited in winter months, and that decaying rice straw is a key driver in C supply.

Decaying rice straw was also a potential source of Hg in winter months, as 86 to 100% of the initial Hg pool was released after the 28-day laboratory incubation (Table 4). However, the relative influence of the THg released by leaf tissue decay was questionable. The THg pool is small compared to the surface (0–2 cm) sediment THg pools (5240 to 6270 $\mu\text{g m}^{-2}$), but comparable in magnitude to reactive sediment Hg(II)_R pools (44 to 120 $\mu\text{g m}^{-2}$, Marvin-DiPasquale et al. this issue). If winter MeHg production occurs predominantly within the anoxic surface liter (e.g. O horizon) then the significance of this pool may be elucidated with further research.

4.4. Biotic exposure and transport by seed consumption

We estimated that the average daily amount of seeds required for waterfowl over-wintering in the Central Valley of California were between 141 to 196 g/day depending on the seed type (Table 5), based on the average waterfowl's daily existence energy requirements and the true metabolizable energy for each seed type for waterfowl (Miller and Eadie, 2006; Heitmeyer, 2010). Our estimates of daily food requirements for an average waterfowl in the Central Valley are similar to other, more detailed, studies on northern pintails (*Anas acuta*; Miller and Newton, 1999; Ballard et al., 2004). We then used these food requirements and our average THg and MeHg concentrations for each seed type to calculate the amount of Hg bioaccumulated daily by waterfowl. We assumed waterfowl diets were entirely composed of a single unhusked seed type for these calculations. Seed production was sufficient to support this level of seed grazing as seed biomass values ranged from 11 to 65 $\text{g}_{\text{dw}} \text{m}^{-2}$ in agricultural fields.

Based on these assumptions, we estimated that waterfowl ingest 7314 ng of THg and 611 ng of MeHg per day when foraging on white rice seeds, 1924 ng of THg and 883 ng of MeHg per day when foraging on wild rice seeds, and 25,473 ng of THg and 213 ng of MeHg per day when foraging on moist-soil seeds (such as swamp timothy and umbrella sedge). Interestingly, the fraction of Hg in the more toxic and bioaccumulative form (MeHg) was highest in wild rice seeds (46%), and lowest in seeds of moist-soil plants (1%) and white rice (8%), suggesting that MeHg exposure to waterfowl will depend largely on their specific diet. A waterfowl diet based entirely on white rice seeds rather than moist-soil seeds results in nearly a 3-fold

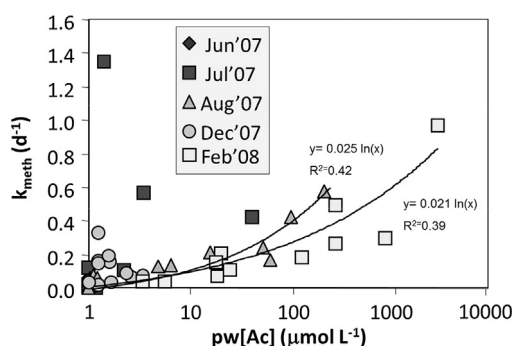


Fig. 4. Log-linear plot of sediment pore water acetate concentration versus the mercury methylation rate constant, by sampling period. Significant non-linear relationships were observed for the peak of the growing season (August 2007; $y = 0.025 \ln(x)$, $r^2 = 0.42$, $p = 0.0018$) and for the mid-winter period during rice-straw decay (February 2008; $y = 0.021 \ln(x)$, $r^2 = 0.39$, $p = 0.0045$).

increase in MeHg exposure, and a 4-fold increase for a diet based on wild rice. This may represent a significant uptake of MeHg by waterfowl who consume mainly rice seeds while overwintering in the Central Valley of California. For example, Miller (1987) found that northern pintail foraged almost exclusively on rice in the Central Valley during August and September, but then foraged on much more moist-soil seeds (e.g. swamp timothy, *Cryptis schoenoides*) and invertebrates later in the winter. Future studies should determine THg and MeHg concentrations in other common moist-soil seeds because our study was limited in scale and included only bulrush (tule) and cattail seeds, which are not typically the most common moist-soil seeds in waterfowl diets (Miller et al., 2009).

Since our data were collected for rice seeds produced during summer, it is unclear whether waterfowl over-wintering in the Central Valley from October through February would be similarly exposed by residual rice seeds. However, our rather limited data in the winter showed no difference between THg and MeHg concentrations in white rice seeds between August and December (THg: Field: $F_{1,11} = 0.01$, $p = 0.96$; Time Period: $F_{1,11} = 0.01$, $p = 0.95$; MeHg: Field: $F_{1,11} = 1.42$, $p = 0.26$; Time Period: $F_{1,11} = 1.44$, $p = 0.26$). Perhaps, more importantly, the bioavailability of Hg species in the husk of rice seeds may be limited due to its indigestibility, and thus the biotic exposure may be lower than calculated for whole seeds, which include husks.

With MeHg:THg ratios in rice and wild rice ranging from 8 to 60%, our results for Hg concentrations in white and wild rice seed is similar to recent studies in China, which found that 11 to 47% of the THg in white rice seed is in the toxic MeHg form. Whereas seed MeHg concentrations were found as high as 32 ng g^{-1} in regions with active artisanal mining (Zhang et al., 2010; Meng et al., 2010), maximal concentrations in white rice of the Yolo Bypass Wildlife Area were only 7 ng g^{-1} . Using data from Feng et al. (2008), geometric means of THg and MeHg concentrations in white rice seeds however were comparable, between the Washan mining province and the Yolo Bypass Wildlife Area (THg = 36 vs. 50 ng g^{-1} ; MeHg = 8.5 vs. 4.2 ng g^{-1}).

The importance of rice crops in California's Central Valley as a significant source of MeHg to humans is likely negligible due to lower rice consumption among local communities (Feng et al., 2008). Further, husk removal in our study was potentially incomplete for white rice seeds, and thus, the white rice seed concentrations reported here may overestimate the concentration in commercially-processed rice seeds. However, the MeHg produced in rice-field soils appears to accumulate to higher concentrations in rice seeds than other wetland seeds and may expose wildlife to Hg, especially waterfowl and shorebirds which use rice-field habitats heavily in the winter and summer for foraging and breeding (Eadie et al., 2008). If we extrapolate our estimated daily exposure of THg to waterfowl to the entire over-wintering period (approximately 5 months), then individual waterfowl feeding exclusively on white rice seeds could be exposed to $1097 \mu\text{g}$ of THg. Speculating further to the entire over-wintering population of waterfowl in the Central Valley of California (approximately 3 million ducks, geese, and swans or 450 million waterfowl use days; Baldassarre and Bolen, 2006), then waterfowl could be exposed to, and removing, approximately 3.3 kg of THg from rice fields each year. Using our limited data to scale to the Central Valley's 225,000 hectares of rice agriculture, seed harvest alone may export 14.3 kg of THg annually from agricultural lands. These rough estimates show that plant uptake and translocation into rice seed should be considered in biotic and harvest fluxes of THg from agricultural wetlands. Future refinements of these estimates should include larger data samples and incorporate the proportional use of rice seeds versus other food types by waterfowl (Brochet et al., 2009).

5. Conclusion

The role of vegetation in MeHg dynamics varied seasonally. Rapid plant growth was associated with relatively labile carbon pools, which decayed quickly upon post-harvest flooding. Total Hg in leaf tissues declined through the growing season, and were significantly correlated with C:N ratios. Methyl Hg in leaf tissues generally increased from summer to fall, and were correlated with root MeHg concentrations, suggesting proportional uptake from soil MeHg pools. Tissue MeHg concentrations were generally greater in seeds than leaves for all species studied, especially white rice and wild rice (4 to 6 ng g^{-1}). Uptake of MeHg into wetland vegetation (macrophyte) biomass (2 to $51 \text{ ng m}^{-2} \text{ d}^{-1}$) played a minor role in seasonal storage of MeHg produced within fields (1 to 2%), but a significant role when compared to rates of hydrologic export (up to 18%). As biomass increased, MeHg storage in aboveground tissues also increased. While these pools of THg and MeHg in plant biomass were 10 - to 100 fold lower than surface sediment pools (0 to 2 cm depth), they temporarily influenced MeHg export as a relatively small sink. Post-season MeHg production was greatest where senescent biomass (litter) was most abundant and labile, a distinct condition of rice-cropped wetlands. Thus, across a full crop year, white rice and wild rice agriculture promoted winter MeHg production, and biotic exposure of Hg species through seed production. With increased cropping and increased atmospheric Hg deposition globally, further attention to ecosystem-level Hg cycling in rice and other flooded agricultural systems is warranted.

Table 5

Estimated biotic uptake of mercury and methylmercury by pintails (*Anas acuta*) using seed-based diet calculations. TME = true metabolizable energy of seeds in kJ d^{-1} for white rice (Reinecke et al., 1989), wild rice (Sherfy, 1999), and common moist soil plants (Reinecke et al., 1989; Checkett et al., 2002). RMR = resting metabolic rate of the average waterfowl present (weight of 1.3 kg) in the Central Valley of California during winter months (Miller and Eadie, 2006). DEE = daily existence energy of a free-living waterfowl was estimated to be 4-times the resting metabolic rate of waterfowl (review by Heitmeyer, 2010).

Plant seed type	Seed TME kJ g^{-1}	Waterfowl RMR kJ d^{-1}	Waterfowl DEE kJ d^{-1}	Food required g d^{-1}	Mean THg ng d^{-1}	SD THg ng d^{-1}	Mean MeHg ng d^{-1}	SD MeHg ng d^{-1}	%MeHg
White rice	13.98	512	2048	146	7314	2250	611	78	8.4
Wild rice	14.52	512	2048	141	1924	985	883	199	45.9
Moist soil	10.46	512	2048	196	25473	6399	213	57	0.8

Acknowledgments

The authors wish to thank the State Water Resources Control Board for financial support, and land managers of the Yolo Bypass for broad access and field support, especially the California Department of Fish and Game (David Feliz) and Jack DeWit of DeWit farms. In addition to initial reviews by JoAnn Holloway (U.S.G.S.), four anonymous reviewers provided substantial comments that greatly improved the manuscript. This publication has been approved by the. We thank Cayce Gulbransen (USGS, Denver) for plant tissue carbon and nitrogen analyses, as well as Mark Rollog (USGS, Menlo Park) for providing independent verification of tissue specific C and N ratios. We thank Allison Lorenzi for providing supplemental analyses of metal and silicon concentrations through ICP-AES. We thank many field and laboratory technicians for both initial experimental set up and for continued sampling and processing during the 1 year study, including Sherrie Wren, Steven Quistad, Justin Kanerva, and Kathy Akstin. The use of trade, product, or firm names in this publication is for descriptive purposes only and does not imply endorsement by the U. S. Government.

References

- Ackerman JT, Eagles-Smith CA. Agricultural wetlands as potential hotspots for mercury bioaccumulation: experimental evidence using caged fish. *Environ Sci Technol* 2010;44:1451–7.
- Ackerman JT, Miles AK, Eagles-Smith CA. Invertebrate mercury bioaccumulation in permanent, seasonal, and flooded rice wetlands within California's Central Valley. *Sci Total Environ* 2010;408:666–71.
- Alpers CN, Fleck J, Stephenson M. Mercury cycling in agricultural and managed wetlands, Yolo Bypass, California: spatial and seasonal variations in water quality. *Sci Total Environ* 2013e. [this issue].
- Bachand PAM, Bachand S, Fleck JA, Anderson F, Alpers CN, Stephenson M. Hydrologic analysis of shallow water cropping systems using reactor models and native tracers: the importance of transpiration in flow path distribution; 2013a [this issue-a].
- Bachand PAM, Bachand SM, Fleck J. Methylmercury production and export from agricultural wetlands (rotational rice) in California, USA: revelations from hydrologic analyses; 2013b [this issue-b].
- Baldassarre GA, Bolen EG. Waterfowl ecology and management. NY: Krieger Publishing; NY; 2006.
- Ballard BM, Thompson JE, Petrie MJ, Chekett M, Hewitt DG. Diet and nutrition of northern pintails wintering along the southern coast of Texas. *J Wildl Manag* 2004;68:371–82.
- Bird JA, van Kessel C, Horwath WR. Stabilization of ¹³C-carbon and immobilization of ¹⁵N-nitrogen from rice straw in humic fractions. *Soil Sci Soc Am J* 2003;67:806–16.
- Brisson J, Chazarenc F. Maximizing pollutant removal in constructed wetlands: should we pay more attention to macrophyte species selection? *Sci Total Environ* 2008;307:3923–30.
- Brochet AL, Guillemin M, Fritz H, Gauthier-Clerc M, Green AJ. The role of migratory ducks in the long-distance dispersal of native plants and the spread of exotic plants in Europe. *Ecography* 2009;32:919–28.
- Brouder SM, Volenec JJ. Impact of climate change on crop nutrient and water use efficiencies. *Physiol Plant* 2008;133:705–24.
- Checkett JM, Drobney RD, Petrie MJ, Graber DA. True metabolizable energy of moist-soil seeds. *Wildl Soc Bull* 2002;30:1113–9.
- Cheng S, Johnson DW, Fu S. Rhizosphere effects on decomposition: controls of plant species, phenology, and fertilization. *Soil Sci Soc Am J* 2003;67:1418–27.
- Devevre O, Horwath WR. Decomposition of rice straw and microbial carbon use efficiency under different soil temperatures and moistures. *Soil Biol Biochem* 2000;32:1773–85.
- DeWild J, Olund SD, Olson ML, Tate MT, DeWild J, Olund SD, et al. Methods for the preparation and analysis of solids and suspended solids for methylmercury: U.S. geological survey techniques and methods for water investigations, book 5; 2004A-7 [21 pp. <http://pubs.usgs.gov/tm/2005/tm5A7/>].
- Eadie JM, Elphick CS, Reinecke K, Miller MR. Wildlife values of North American ricelands. In: Manley SW, Petrie M, Batt BJ, editors. Conservation in ricelands of North America: current state of our knowledge and a course for future research and education. Memphis, TN: Institute for Waterfowl and Wetlands Research, Ducks Unlimited; 2008. p. 7–90.
- Ehrenfeld JG, Ravit B, Elgersma K. Feedback in the plant–soil system. *Ann Rev Environ Resour* 2005;30:75–115.
- Erickson JA, Gustin MS. Foliar exchange of mercury as a function of soil and air mercury concentrations. *Sci Total Environ* 2004;324:271–9.
- Fay L, Gustin MS. Investigation of mercury accumulation in cattails growing in constructed wetland mesocosms. *Wetlands* 2007;27:1056–65.
- Feng X, Li P, Qiu G, Wang S, Li G, Shang L, et al. Human exposure to methylmercury through rice intake in mercury mining areas, Guizhou Province, China. *Environ Sci Technol* 2008;42:326–32.
- Fleck JA, Gill G, Downing BD, Bergamaschi BA, Kraus TEC, Downing BD, et al. Concurrent photolytic degradation of aqueous methylmercury and dissolved organic matter; 2013. <http://dx.doi.org/10.1016/j.scitotenv.2013.03.017> [in press].
- Gabrielsen GW, Mehlum F, Karlsen HE, Andresen O, Parker H. Energy cost during incubation and thermoregulation in the female common eider *Somateria mollissima*. *Nor Polarinst* 1991;195:51–62.
- Grace JB, Wetzel RG. Long-term dynamics of *Typha* populations. *Aquat Bot* 1998;61:137–46.
- Gu L, Post WM, King AW. Fast labile carbon turnover obscures sensitivity of heterotrophic respiration from soil to temperature: a model analysis. *Glob Biogeochem Cycles* 2004;18:GB1022. <http://dx.doi.org/10.1029/2003GB002119>.
- Hall BD, St. Louis VL, Bodaly RA. The stimulation of methylmercury production by decomposition of flooded birch leaves and jack pine needles. *Biogeochemistry* 2004;68:107–29.
- Heitmeyer ME. A manual for calculating duck-use-days to determine habitat resource values and waterfowl population energetic requirements in the Mississippi Alluvial Valley. Greenbrier Wetland Services Report 10–01. MO: Blue Heron Conservation Design and Printing LLC, Bloomfield; 2010.
- Hines ME, Banta GT, Giblin AE, Hobbie JE, Tugel JB. Acetate concentrations and oxidation in salt-marsh sediments. *Limnol Oceanogr* 1994;39:140–8.
- Iiyama K, Wallis AFA. An improved acetyl bromide procedure for determining lignin in woods and wood pulps. *Wood Sci Technol* 1988;22:271–80.
- Jacob DL, Otte ML. Conflicting processes in the wetland plant rhizosphere: metal retention or mobilization? *Water Air Soil Pollut* 2003;3:91–104.
- Lamers LPM, Van Diggelen JMH, Op den Camp HJM, Visser EFW, Lucassen ECHET, Vile MA, Jetten MSM, Smolders AJ, Roelofs JGM. Microbial transformations of nitrogen, sulfur, and iron dictate vegetation composition in wetlands: a review. *Frontiers in Microbiology* 2012;3:1–12. <http://dx.doi.org/10.3389/fmicb.2012.00156>.
- Lee R, Kraus DW, Doeller JE. Oxidation of sulfide by *Spartina alterniflora* roots. *Limnol Oceanogr* 1999;44:1155–9.
- Leonard TL, Taylor GE, Gustin MS, Fernandez GCJ. Mercury and plants in contaminated soils: 1. Uptake, partitioning, and emission to the atmosphere. *Environ Toxicol Chem* 1998;17:2063–71.
- Marchand L, Mench M, Jacob DL, Otte ML. Metal and metalloid removal in constructed wetlands, with emphasis on the importance of plants and standardized measurements: a review. *Environ Pollut* 2010;158:3447–61.
- Marschner H. The mineral nutrition of higher plants. 2nd ed. London: Academic Press; 1995 [889 pp.].
- Marvin-DiPasquale MC, Windham-Myers L, Agee JL, Kakouros E, Kieu LH, Fleck JA. Methylmercury production in sediment from agricultural and non-agricultural wetlands in the Yolo Bypass, California; 2013e [this issue].
- Melillo JM, Aber JD, Muratore JM. Nitrogen and lignin control of hardwood leaf litter decomposition dynamics. *Ecology* 1982;63:621–6.
- Meng B, Feng X, Qiu G, Cai Y, Wang D, Li P, et al. Distribution patterns of inorganic mercury and methylmercury in tissues of rice (*Oryza sativa* L.) plants and possible bioaccumulation pathways. *J Agric Food Chem* 2010;58:4951–8.
- Miller MR. Fall and winter foods of northern pintails in the Sacramento Valley, California. *J Wildl Manag* 1987;51:405–14.
- Miller MR, Eadie JMCA. The allometric relationship between resting metabolic rate and body mass in wild waterfowl (Anatidae) and an application to estimation of winter habitat requirements. *Condor* 2006;108:166–77.
- Miller MR, Newton WE. Population energetics of northern pintails wintering in the Sacramento Valley, California. *J Wildl Manag* 1999;63:1222–38.
- Miller MR, Burns EG, Wickland BE, Eadie JM. Diet and body mass of wintering ducks in adjacent brackish and freshwater habitats. *Waterbirds* 2009;32:374–87.
- Mitsch WJ, Nahlik AM, Wolski P, Bernal B, Zhang L, Ramberg L. Tropical wetlands: seasonal hydrologic pulsing, carbon sequestration, and methane emissions. *Wet Ecol Manag* 2010;18:573–86.
- Patra M, Sharma A. Mercury toxicity in plants. *Bot Rev* 2000;66:379–422.
- Patty C, Barnett B, Mooney B, Kahn A, Levy S, Liu Y, et al. Using X-ray microscopy and Hg L3 XANES to study Hg binding in the rhizosphere of *Spartina* cordgrass. *Environ Sci Technol* 2009;43:7397–402.
- Reinecke KJ, Kaminski RM, Moorhead DJ, Hodges JD, Nassar JR. Mississippi alluvial valley. In: Smith LM, Pederson RL, Kaminski RM, editors. Habitat management for migrating and wintering waterfowl in North America. Lubbock, USA: Texas Tech University Press; 1989. p. 203–47.
- Rocha AV, Potts DL, Goulden ML. Standing litter as a driver of interannual CO₂ exchange variability in a freshwater marsh. *J Geophys Res Biogeosci* 2008. <http://dx.doi.org/10.1029/2008JG000713>.
- Rothenberg SE, Feng X. Mercury cycling in a flooded rice paddy. *J Geophys Res Biogeosci* 2012;117:G03003. <http://dx.doi.org/10.1029/2011JG001800>.
- Rothenberg SE, Feng X, Zhou W, Tu M, Jin B, You J. Environment and genotype controls on mercury accumulation in rice (*Oryza sativa* L.) cultivated along a contamination gradient in Guizhou, China. *Sci Total Environ* 2012;426:272–80.
- Schwesig D, Krebs O. The role of ground vegetation in the uptake of mercury and methylmercury in a forest ecosystem. *Plant Soil* 2003;253:445–55.
- Sereno DM, Stacey M. Turbulence, bottom boundary conditions, and sediment transport in a shallow water habitat. In: Wohl, et al, editor. Hydraulic measurements and experimental methods. Reston, VA: American Society of Civil Engineers; 2002. [1111 pp.].
- Sherfy MH. Nutritional value and management of waterfowl and shorebird foods in Atlantic Coastal moist-soil impoundments. Dissertation Blacksburg, Virginia, USA: Virginia Poly-technic Institute and State University; 1999.
- Springborn M, Singer MB, Dunne T. Sediment-adsorbed total mercury flux through Yolo Bypass, the primary floodway and wetland in the Sacramento Valley, California. *Sci Total Environ* 2011;412:203–13.

- Stamenkovic J, Gustin MS. Non-stomatal versus stomatal foliar mercury exchange. *Environ Sci Technol* 2009;43:1367–72.
- Stein ED, Cohen Y, Winer AM. Environmental distribution and transformation of mercury compounds. *Crit Rev Environ Sci Technol* 1996;26:1–43.
- TIBCO. Spotfire S-Plus 8.1. Palo Alto, CA: TIBCO Software, Inc.; 2008.
- Weis JS, Windham L, Weis P. Patterns of metal accumulation in leaves of the tidal marsh plants *Spartina alterniflora* Loisel and *Phragmites australis* Cav. Trin ex Steud. Over the growing season. *Wetlands* 2003;23:459–65.
- Windham-Myers L, Marvin-DiPasquale M, Krabbenhoft DP, Agee JL, Cox MH, Heredia-Middleton P, Coates C, Kakouros E. Experimental removal of wetland emergent vegetation leads to decreased methylmercury production in surface sediments. *Journal of Geophysical Research* 2009;114:G00C05. <http://dx.doi.org/10.1029/2008JG000815>.
- Windham-Myers L, Ackerman JT, Fleck JA, Marvin-DiPasquale M, Stricker CA, Bachand P, et al. Mercury cycling in agricultural and managed wetlands: a synthesis of observations from an integrated field study of methylmercury production, hydrologic export, and bioaccumulation; 2013a [this issue-a].
- Windham-Myers L, Marvin-DiPasquale M, Stricker C, Agee JL, Kieu L, Kakouros E. Mercury cycling in agricultural and managed wetlands, Yolo Bypass, California: experimental evidence of vegetation-driven changes in sediment biogeochemistry and methylmercury production; 2013b [this issue-b].
- Wollenberg JL, Peters SC. Diminished mercury emission from waters with duckweed cover. *J Geophys Res Biogeosci* 2009. <http://dx.doi.org/10.1029/2008JG000770>.
- Zhang H, Feng X, Larssen T, Shang L, Li P. Bioaccumulation of methylmercury versus inorganic mercury in rice (*Oryza sativa* L.) grain. *Environ Sci Technol* 2010;44:449–4504.